Ultrasound in Med. & Biol., Vol. 41, No. 11, pp. 2913–2925, 2015

0301-5629/$ - see front matter

http://dx.doi.org/10.1016/j.ultrasmedbio.2015.06.012

● *Original Contribution*

FLOW VELOCITY MAPPING USING CONTRAST ENHANCED HIGH-FRAME-RATE PLANE WAVE ULTRASOUND AND IMAGE TRACKING: METHODS AND INITIAL *IN VITRO* AND *IN VIVO* EVALUATION

CHEE HAU LEOW,* ELENI BAZIGOU,* ROBERT J. ECKERSLEY,† ALFRED C. H. YU,‡ PETER D. WEINBERG,* and MENG-XING TANG*

*Department of Bioengineering, Imperial College London, London, United Kingdom; †Department of Biomedical Engineering, King's College London, London, United Kingdom; and ‡Medical Engineering Program, University of Hong Kong, Pokfulam, Hong Kong

(*Received* 21 *December* 2014; *revised* 22 *April* 2015; *in final form* 16 *June* 2015)

Abstract—Ultrasound imaging is the most widely used method for visualising and quantifying blood flow in medical practice, but existing techniques have various limitations in terms of imaging sensitivity, field of view, flow angle dependence, and imaging depth. In this study, we developed an ultrasound imaging velocimetry approach capable of visualising and quantifying dynamic flow, by combining high-frame-rate plane wave ultrasound imaging, microbubble contrast agents, pulse inversion contrast imaging and speckle image tracking algorithms. The system was initially evaluated *in vitro* on both straight and carotid-mimicking vessels with steady and pulsatile flows and *in vivo* in the rabbit aorta. Colour and spectral Doppler measurements were also made. Initial flow mapping results were compared with theoretical prediction and reference Doppler measurements and indicate the potential of the new system as a highly sensitive, accurate, angle-independent and full field-of-view velocity mapping tool capable of tracking and quantifying fast and dynamic flows. (E-mail: mengxing.tang@imperial.ac.uk) **© 2015 World Federation for Ultrasound in Medicine & Biology.**

Key Words: **Flow, Microbubble contrast agents, Ultrafast ultrasound imaging, Ultrasound imaging velocimetry, Echo-particle image velocimetry, Atherosclerosis, Image tracking.**

INTRODUCTION

Techniques capable of quantitative mapping blood flow velocity *in vivo* are highly desirable in studying a wide range of cardiovascular diseases. For instance, flow velocity and its derivatives, such as vorticity and wall shear stress, are essential in the study of the pathogenesis of atherosclerosis (Cecchi et al. 2011; Davies 2009). Existing non-invasive techniques for flow velocity mapping have various limitations. For example, phase-contrast magnetic resonance imaging (MRI) and phase velocity mapping are valuable clinical modalities that offer the potential to obtain volumetric velocity vectors *in vivo*. However, the low temporal resolution and lack of accessibility (Reneman et al. 2006; Yim et al. 2005) may limit their application for routine clinical use. Doppler ultrasound is used extensively for visualization and measurement of blood flow clinically (Evans et al. 2011; Hoskins 1997; Steel et al. 2003); the blood velocity is calculated from the changes in either frequency or phase of the ultrasound reflected from moving red blood cells. However, in most existing ultrasound scanners, images are formed line by line, resulting in an inherent trade-off between field of view and Doppler sensitivity or frequency resolution. Additionally, because of the weak scattering from blood cells, Doppler also has a trade-off between spatial/temporal resolution and signal-to-noise ratio (SNR). The performance can also be affected by various artifacts because of aliasing and beam-flow angle variations (Evans and Wells 2010). Some new Doppler techniques have been developed, including crossed-beam vector Doppler (Kripfgans et al. 2006; Pastorelli et al. 2008; Ricci et al. 2014; Tortoli et al. 2010), vector flow mapping (Ohtsuki and Tanaka 2006; Uejima et al. 2010), directional cross-correlation method (Jensen and Lacasa 1999; Kortbek and Jensen 2006), transverse oscillation method (Pedersen et al. 2014; Udesen and Jensen 2006), and pulse inversion Doppler (Simpson et al.

Address correspondence to: Meng-Xing Tang, Department of Bioengineering, Imperial College London, South Kensington Campus, London SW7 2AZ, UK. E-mail: mengxing.tang@imperial.ac.uk

1999; Tremblay-Darveau et al. 2014). Non-Doppler ultrasound techniques have also been investigated. Speckle image velocimetry (SIV) is a quantitative flow mapping technique combining high-frequency ultrasound imaging with cross-correlation analysis (Bohs et al. 2000). It generates accurate flow vectors by tracking the speckle patterns scattered by red blood cells (RBCs) in B-mode images. Although studies have reported the feasibility of using SIV to provide accurate flow mapping (Fadnes et al. 2014; Nam et al. 2012; Swillens et al. 2010a), the application is still limited by the low SNR of the scattering from RBCs (Yeom et al. 2014) and would be especially difficult for low-frequency imaging of deeper vessels. Swillens et al. (2010b) compared vector Doppler and speckle tracking for quantifying blood flow using line-by-line scanning ultrasound and concluded that high-frame-rate plane wave ultrasound would address the current limitations of both approaches.

Microbubble contrast agents are able to significantly enhance ultrasound signals from within the blood, offering substantial benefit for quantitative ultrasound imaging of flow and perfusion (Sboros et al. 2010; Stride et al. 2009; Tang et al. 2011). These microbubbles, typically between 1 and 7 μm in size and encapsulated with lipid, albumin or other surfactants, have been used in a range of clinical applications in cardiology and radiology and have great potential for molecular imaging and therapy (Ferrara et al. 2007; Lindner 2004, 2009; Stride and Coussios 2010).

Taking advantage of microbubble contrast agents, ultrasound imaging velocimetry (UIV, also called echo-particle image velocimetry) is a non-Doppler method that tracks speckles scattered from within blood by microbubbles, providing a new tool to accurately measure the blood flow field. Similar to optical PIV, which is widely used in flow accessible with an optically transparent window (Adrian and Westerweel 2011), a cross-correlation algorithm is typically used to identify and track ultrasound speckle features in consecutive frames of an image sequence and obtain displacement vectors within the image. Given such vectors and the imaging frame rate, the velocity vector can be obtained. Studies using UIV have shown great promise in imaging vascular flow (Nam et al. 2012; Poelma et al. 2009, 2012; Qian et al. 2010; Zhang et al. 2011). However, existing UIV systems use clinical ultrasound imaging systems that perform line-by-line scanning, causing errors in UIV velocity estimation and significantly limiting the maximum velocity and acceleration such scanning systems can track (Zhou et al. 2013).

Recent developments in high-frame-rate ultrasound imaging technology offer new possibilities for flow estimation. By transmitting unfocussed ultrasound pulses and using parallel receive beamforming instead of line-by-line scanning, substantially higher acquisition rates (up to 20,000 frame/s) can be achieved (Jensen et al. 2006; Montaldo et al. 2009). This fast imaging technique has been proposed for shear wave elastography, electromechanical wave imaging, ultrafast Doppler, ultrafast contrast imaging and functional ultrasound imaging of brain activity (Couture et al. 2009; Tanter and Fink 2014). Notably in flow imaging, fast imaging techniques show promising results, especially in ultrafast Doppler (Bercoff et al. 2011; Jensen and Nikolov 2004) and vector Doppler (Ekroll et al. 2013; Flynn et al. 2012; Lenge et al. 2014; Yiu et al. 2014). The use of high-frame-rate ultrasound to track microbubbles in the bloodstream between imaging frames (high frame-rate UIV) has not been reported.

In this study, our aim was to develop a highly sensitive, accurate, angle-independent and full-field-of-view flow velocity mapping tool capable of tracking fast and dynamic flows, by combining high-frame-rate plane wave ultrasound imaging, ultrasound imaging velocimetry, microbubble contrast agents and pulse-inversion contrast imaging. The system was initially evaluated *in vitro* on flow phantoms with highly dynamic and pulsatile flows and *in vivo* in the rabbit aorta.

METHODS

A high-frame-rate UIV system was developed based on tracking the speckle patterns of microbubble contrast agents in contrast-enhanced ultrasound image sequences acquired from a high-frame-rate plane wave imaging system.

Microbubble contrast agents

Decafluorobutane microbubbles were prepared as described by Sheeran et al. (2011). 1,2-Dipalmitoyl-*sn*-glycero-3-phosphatidylcholine (DPPC), 1,2-dipalmitoyl-*sn*-glycero-3-phosphatidylethanolamine-polyethylene glycol 2000 (DPPE-PEG-2000) and 1,2-dipalmitoyl-3-trimethylammonium propane (chloride salt, 16:0 TAP) were dissolved in a molar ratio of 65:5:30 and total lipid concentrations of 0.75, 1.5 and 3 mg/mL, resulting in a solution composed of 15% propylene glycol, 5% glycerol and 80% normal saline. Microbubbles were generated *via* agitation of a 2-mL sealed vial containing 1.5 mL of the resulting solution, using a shaker, for 60 s.

The microbubble solution generated was sized and counted according to Sennoga et al. (2012) and was found to have a concentration of about 5×10^9 microbubbles/mL with an average size of 1 μm. In this study, microbubbles were diluted in gas-equilibrated water (Mulvana et al. 2012) to a concentration of 2×10^5 microbubbles/mL, a clinically relevant concentration as used in previous studies (Tang et al. 2010).

Fast ultrasound imaging system and pulse inversion

A L12-3 v linear array probe connected to a Vantage 128 research platform (Verasonic, Redmond, WA, USA) was used to acquire high-frame-rate ultrasound images, as illustrated in Figure 1. Because the platform consists of 128 transmit and receive channels, 128 elements located at the centre of the 192-element probe were used in each pulse-echo sequence, resulting in a 25-mm lateral field of view. A plane wave pulse-inversion imaging scheme was used to acquire contrast images. Twelve plane waves with six angles tilted between −18° and +18° (7.2° step) were transmitted with a pulse repetition frequency of 15.5 kHz to form an image after coherent compounding (Montaldo et al. 2009), achieving a frame rate of 1000 Hz for an imaging depth of 25 mm. For each angle, a 3-MHz 1-cycle plane wave pulse followed by its phase-inverted counterpart (pulse inversion) was transmitted while the radiofrequency (RF) echoes were recorded in local memory. The RF data collected were then transferred back to a computer through a high-speed PCI-Express and software beamformed into images for further analysis using MATLAB (The MathWorks, Natick, MA, USA).

UIV analysis

Ultrasound imaging velocimetry analysis of the acquired images was performed based on Niu et al. (2010). This well-established method is a modification of the conventional PIV algorithm (Adrian 1991) illustrated in Figure 2 and incorporates several improvements, including a multiple iterative algorithm, subpixel method, filter and interpolation method and spurious vector elimination algorithm to improve the accuracy of the measurement (Niu et al. 2010). A universal outlier detection

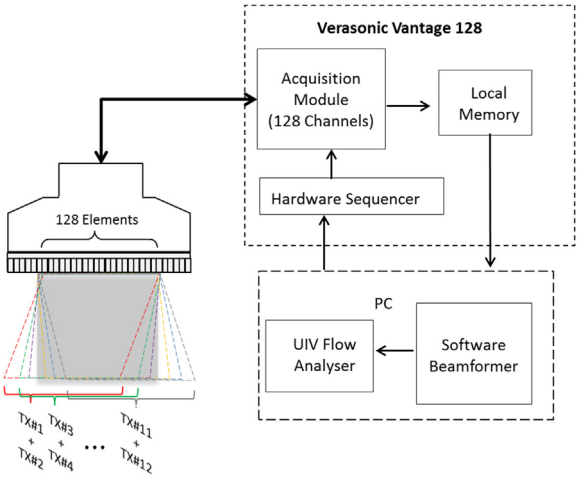

Fig. 1. Overview of the system hardware and data acquisition scheme involve in plane wave UIV. UIV = ultrasound imaging velocimetry.

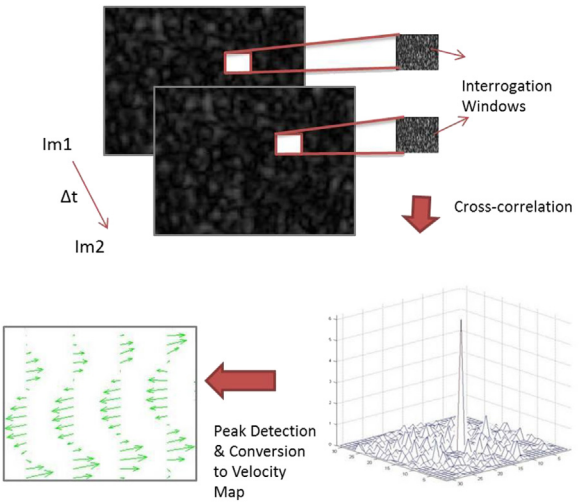

Fig. 2. Principle underlying conventional particle image velocimetry: Two consecutive ultrasound images were divided into several interrogation windows. For each window, cross-correlation analysis was performed to compute a local velocity displacement. The location of the peak within the correlation map was identified and displayed on the velocity map.

method as described by Westerweel and Scarano (2005) was also implemented to eliminate spurious vectors.

Straight-vessel flow phantom

To evaluate the system, *in vitro* experiments on a straight-vessel phantom were performed, and measurements made with plane wave UIV were compared with both analytically derived values and ultrasound Doppler under various flow conditions. The flow system was constructed as illustrated in Figure 3. A 6-mm latex tube (098 XA/XB, Pipeline Industries, Denver, CO, USA) was placed in a water tank filled with gas-equilibrated water. The L12-3v transducer mounted on a Verasonics Platform was placed above the tube to acquire the contrast images, and an 11 L4 transducer mounted on a Toshiba ultrasound system (AplioXG, Toshiba Medical Systems, Otawara, Japan) was placed 5 cm away from the L12-3v transducer to acquire Doppler measurements. Both transducers were tilted at an angle of 8° to the flow

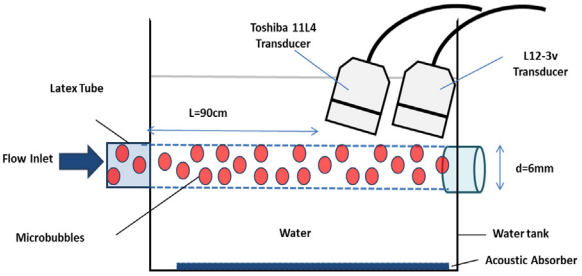

Fig. 3. Schematic of the straight-tube flow system.

Table 1. Flow parameters of three different laminar flows

Flow condition	Measured flow rate (mL/min)	V_{max} (cm/s)	Re
Slow	85	10	300
Medium	325	38	1200
Fast	500	59	1768

direction, but were operated alternately to avoid interference. An acoustic absorber was placed at the bottom of the tank to prevent reflection from the tank walls.

Steady laminar flow. A gravity flow setup was employed to create a steady laminar flow through the latex tube at a constant rate. The working fluid flow through the tube was a diluted microbubble solution that had been mixed uniformly by manual stirring at the source tank before the experiment began. Both transducers were placed more than 70 cm away from the inlet to measure a region where a fully developed laminar flow with parabolic velocity profile could be observed. The inlet length was calculated with the formula taken from McDonald (1974): $L = 0.04d$ Re, Re $= Vdp/u$, where d is the diameter of the tube, Re is the Reynold's number, V is the average velocity, p is the fluid density and u is the dynamic viscosity.

Measurements were obtained at three flow rates, as outlined in Table 1. A series of contrast images were acquired at a 1000-Hz frame rate using the Verasonics platform and analysed using the UIV algorithm. The results were then compared with the analytical velocity profile calculated on the basis of the measured average flow rate using a bucket and stopwatch. Also, colour Doppler and spectral Doppler velocities located at the centre of the tube were recorded using the Toshiba ultrasound system.

Pulsatile flow. Pulsatile flow was investigated with the same experimental setup. The pulsatile flow of 80 strokes/min, delivering 4 mL solution/stroke, was driven by a pulsatile pump (Harvard Apparatus 1405 pulsatile blood pump, Harvard Apparatus, Kent UK). Plane wave contrast images were obtained and post-processed using the UIV algorithm; the trimode Doppler measurements were obtained using the Toshiba scanner.

In vitro *carotid bifurcation model investigation*

An anatomically realistic carotid bifurcation model as described in Lai et al. (2013) was used to further evaluate the system. The phantom vessel contains three branches mimicking, in turn, the common carotid artery (CCA), the internal carotid artery (ICA) and the external carotid artery (ECA). The experimental setup and normal carotid bifurcation model are illustrated in Figure 4. Instead of using water, microbubbles were diluted in a blood-mimicking fluid (BMF), which comprised 90% pure water and 10% glycerol, to reflect a physiologic relevant condition (Ramnarine et al. 1998). The inlet of the setup was connected to a pulsatile pump (Harvard Apparatus 1405 pulsatile blood pump), delivering 3 mL of the diluted microbubble solution per stroke and running at 80 strokes/min.

In vivo *rabbit experiment*

Experiments were conducted to measure blood flow velocities in the abdominal aorta of the rabbit *in vivo*, as illustrated in Figure 5. All procedures complied with the Animals (Scientific Procedures) Act 1986 and were approved by the Local Ethical Review Process Committee of Imperial College London. A male New Zealand White rabbit (1.5 y old) was anaesthetised with medetomidine (0.25 mL/kg) and ketamine (0.15 mL/kg) and its body temperature maintained at 37°C by a warming plate. With the fur around the scanning site removed, images of the rabbit's abdominal aorta were acquired non-invasively using the Verasonics system and an L12-3v probe while a bolus of 0.1 mL Sonovue microbubbles

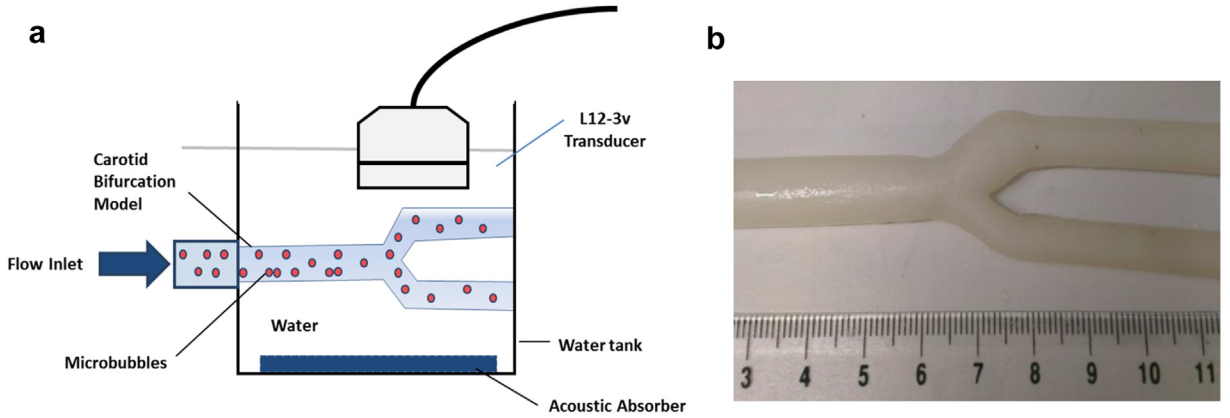

Fig. 4. (a) Schematic of the carotid bifurcation experimental setup. (b) Carotid bifurcation tube without stenosis.

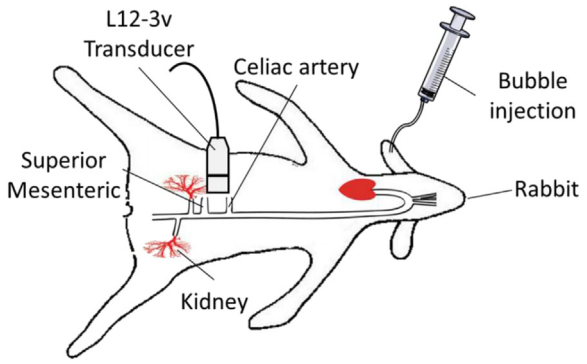

Fig. 5. *In vivo* experimental setup. Contrast agents were injected through the anaesthetised rabbit's ear, and the rabbit abdominal aorta was scanned using an L12-3 probe.

was injected *via* the marginal ear vein. The ultrasound imaging settings were the same as in the *in vitro* studies.

RESULTS

Straight-vessel phantom

Steady laminar flow. Figure 6 illustrates the comparison between flow measurements acquired using Doppler ultrasound and plane wave UIV. Figure 6(a–f) illustrates the Doppler measurements, and Figure 6(g–l), the plane wave UIV measurements. The Doppler measurements were acquired in triplex mode, where B-mode, colour and spectral Doppler were obtained at the same time. In each measurement, the colour Doppler images show the flow field across the tube while the centerline peak velocity was obtained using spectral Doppler with a 1×1-mm range gate, as illustrated in Figure 6(a–c). In Figure 6(d–f), a *red line* is drawn in each spectral measurement to indicate the maximum velocity in the spectral Doppler measurements. The peak velocities obtained were 12.5, 46 and 68 cm/s; these are slightly higher than the analytical peak velocities derived from the measured flow rates obtained using a bucket and stopwatch, which were 10, 38 and 59 cm/s. The discrepancy is probably due to an imperfect setting of spectral Doppler angle and the broadening of the Doppler spectrum by microbubbles (Tortoli et al. 2009).

The images and data illustrated in Figure 6(g–l) were obtained using plane wave UIV with a 1-kHz acquisition rate. Fully developed laminar flows of parabolic profile under the slow and fast flow conditions in the 6-mm tubes can be clearly visualised. The parabolic flow vectors are consistent across the tube under all flow conditions. To provide a quantitative measurement, the velocity fields were also represented in a colour-encoded vector plot overlaid on the contrast-enhanced images. In all cases illustrated in Figure 6(j–l), plane wave UIV measurements were found to match the analytical flow profile with good accuracy: root mean square errors of 0.66 cm/s (6.6%), 3.64 cm/s (9.6%) and 3.63 cm/s (6.2%) were obtained in slow, medium and fast flow.

Pulsatile flow. With plane wave UIV, the high spatiotemporal dynamics of the pulsatile flow were effectively tracked by plane wave UIV at a 1-ms time resolution, as illustrated in Supplementary Video 1 (see online version at http://dx.doi.org/10.1016/j.ultrasmedbio.2015.06.012). In Figure 7 is the spatial velocity profile measured with Doppler and UIV at different phases of the dynamic flow, marked on a spectral measurement as indicated in Figure 7(m). The colour vector images (Fig. 7e–h) are highly correlated with the colour Doppler measurements (Fig. 7a–d). Flow with a blunt velocity profile moving in the forward direction can be observed during the peak systolic phase in Figure 7(e). This undeveloped flow profile is common in arteries under pulsatile flow conditions when the centreline velocity accelerates as the boundary layer retards velocity near the wall (He and Ku 1994; Ku 1997). After the peak systolic phase, a developed laminar flow can be observed (Fig. 7f). Reversed flow is observed near the vessel wall in Figure 7(g), and a non-uniform forward flow pattern can be seen in Figure 7(h). All these velocity profiles are relevant to the *in vivo* condition in which pulsatile flow applies (Ku 1997). The velocity profiles across the tube at each reference time point are illustrated in Figure 7(i–l). The temporal velocity profile within the same spatial window used by spectral Doppler was also extracted from the plane wave UIV results and overlaid on the spectral Doppler measurement, as illustrated in Figure 7(m). There is a good agreement between the plane wave UIV measurement and the Doppler spectral measurement at the same spatial location.

Carotid bifurcation model

Supplementary Video 2 (see online version at http://dx.doi.org/10.1016/j.ultrasmedbio.2015.06.012) illustrates the temporal evolution of flow patterns in a healthy carotid bifurcation model. In this study, instead of using six-angled plane wave transmissions, contrast images were acquired with three-angled transmissions within the same angle range. By reducing the compounding, the dynamic flow patterns were effectively tracked using the plane wave UIV system with an acquisition rate of 2000 fps and played back at 50 fps. The flow patterns at different time points indicated in Figure 8(g) are illustrated in a collection of images in Figure 8(a–f). Figure 8(a, b) illustrates the forward flow during the acceleration and the peak systolic phase. A vortex is subsequently seen near the vessel wall at the carotid bulb

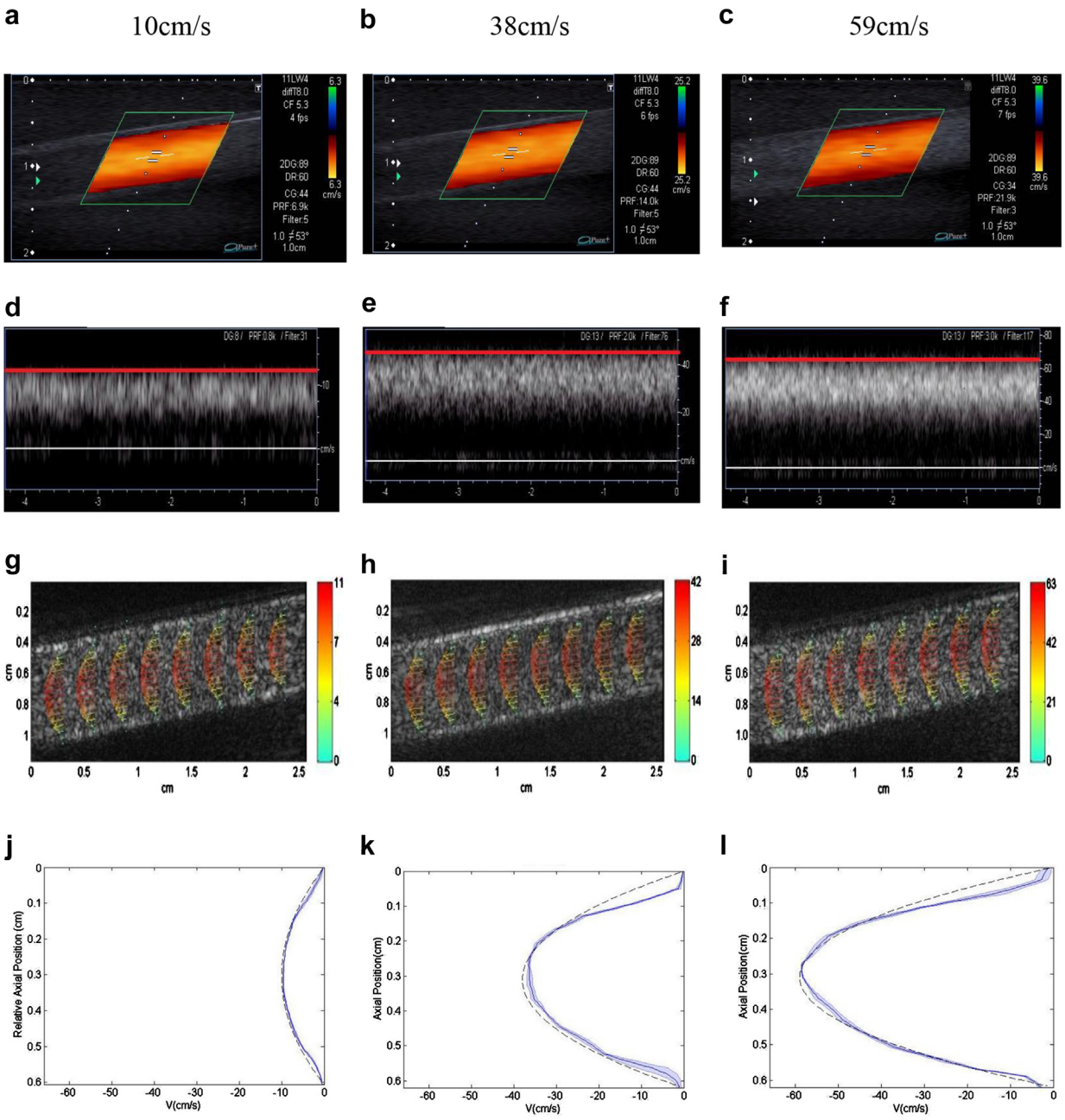

Fig. 6. Comparison of Doppler ultrasound with plane wave UIV at three flow rates with peak velocities of 10, 38 and 59 cm/s. (a–c) Colour Doppler images obtained using standard beam-formed colour Doppler processing. (d–f) Spectral Doppler measurements acquired from the corresponding window located in the colour images. The *red line* indicates the maximum velocity. (g–i) UIV-derived quantitative vector visualisation. Each measurement is averaged over 5 ms. (j–l) Measured flow profiles corresponding to the three flow conditions reveal a high correlation with the analytically derived flow profile (*dashed line*). Note: Results in (j)–(l) were averaged over a 1-mm lateral position, where the *solid line* represents the mean value and the *shading* represents the standard deviation. UIV = ultrasound imaging velocimetry.

during the post-systolic phase (Fig. 8c) and persists during the deceleration phase, as illustrated in (Fig. 8d). The transitory behaviour of the flow can be clearly seen in Supplementary Video 2, in which the vortex appears immediately after peak systole and slowly dissipates until it reaches the peak dicrotic wave, at which moment the flow resumes forward motion again (Fig. 8e). Finally at the end of the dicrotic wave, the vortex near the carotid bulb reappears (Fig. 8f). This finding agrees with those of Yiu et al. (2014).

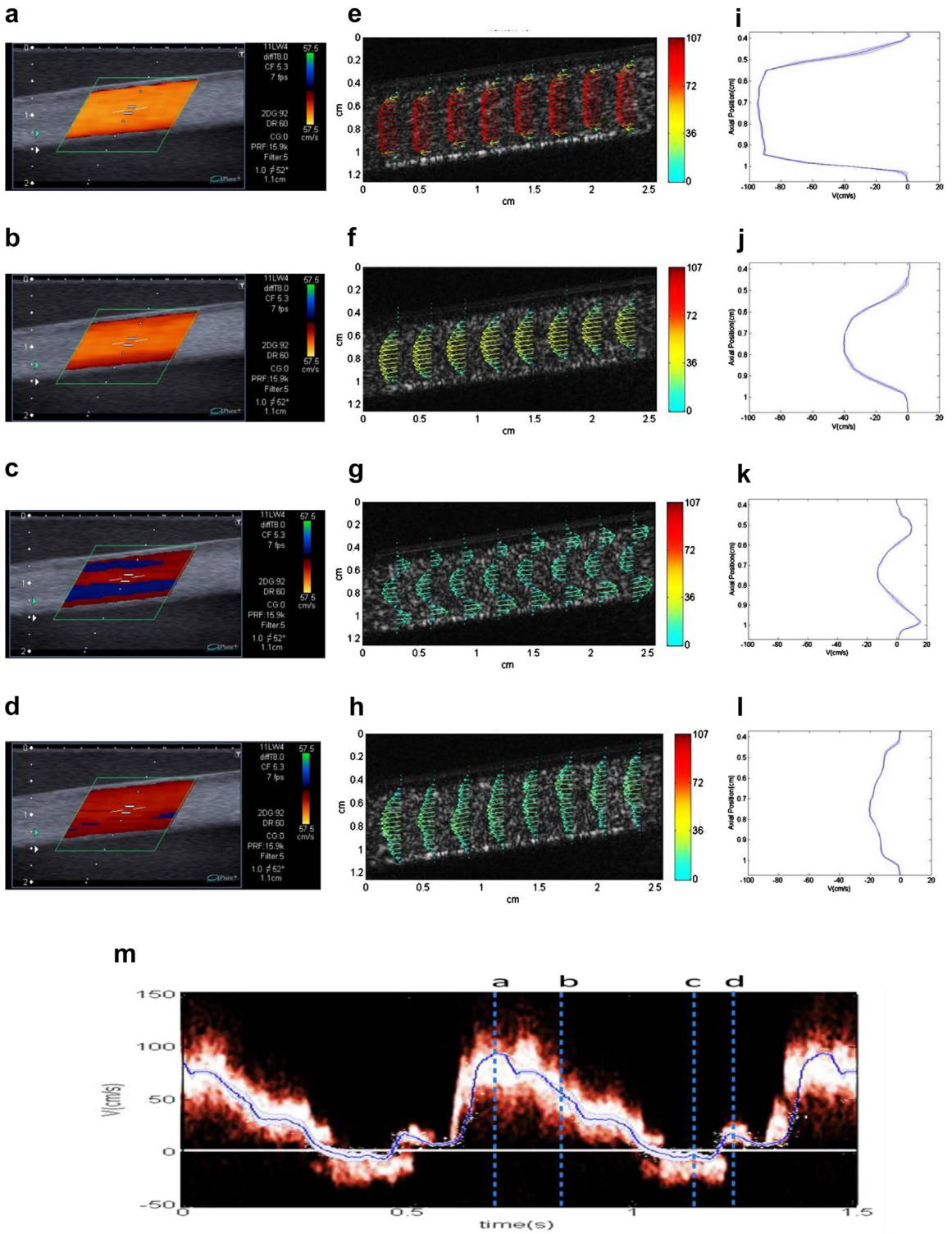

Fig. 7. Visualisation and quantification of pulsatile flow at the four phases indicated by *dotted lines* in (m). (a–d) Colour Doppler measurements acquired at the four different phases. (e–l) Colour vector of flow measurements obtained using plane wave UIV (e–h) and their corresponding flow profiles (i–l). (m) Comparison of centreline velocity obtained from plane wave UIV (*blue line*) with spectral Doppler. Note: Results in (i)–(l) were averaged over a 1-mm lateral position, where the *solid line* represents the mean value and the *shading* represents the standard deviation. Spectral Doppler measurement and plane wave UIV results s in (m) were averaged over a 1 × 1-mm window located at the centre of the vessel. UIV = ultrasound imaging velocimetry.

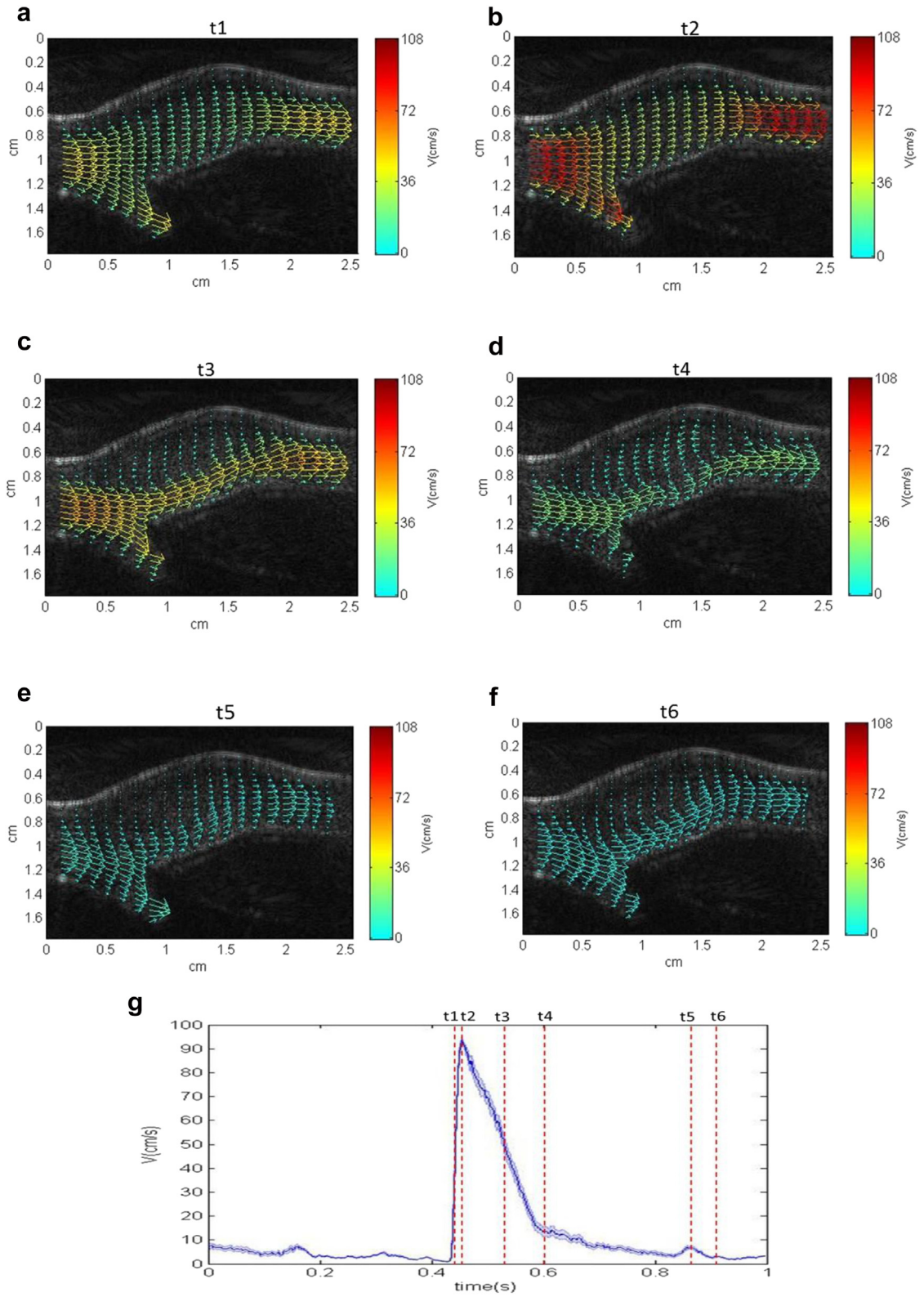

Fig. 8. (a–f) Quantitative visualisation of key flow patterns obtained at different phases under pulsatile conditions in a model of a healthy carotid bifurcation. (g) Centreline velocity obtained using ultrasound imaging velocimetry from a 1 × 1-mm range gate located within the common carotid artery. The relative position of each flow pattern is marked in the velocity plot.

In vivo *rabbit experiment*

The flow patterns obtained in the rabbit abdominal aorta (between the celiac artery and superior mesenteric artery) during one pulse cycle with three-angled plane wave compounding and a frame rate of 2.5 kHz are illustrated in Figure 9 and Supplementary Video 3 (see online version at http://dx.doi.org/10.1016/j.ultrasmedbio.2015.06.012). Forward flow can be observed in Figure 9(a, c, d), whereas reversed flow, and additionally a vortex, can be seen in Figure 9(b). This finding agrees with the results of Yamaguchi et al. (1987) and Gulan et al. (2012).

In addition, an initial qualitative comparison of the result obtained from the developed system and the Doppler systems is provided in Figure 10. With the 2-kHz acquisition rate, the spatiotemporal flow variations over a wide range of velocities were well tracked using plane wave UIV, and the estimations in Figure 10(b) were found to match the Doppler measurement (Fig. 10a). However, it should be noted that as a result of the angle dependence of the Doppler measurement, the highest flow velocity in the aorta appears slower than that in the branch (renal artery).

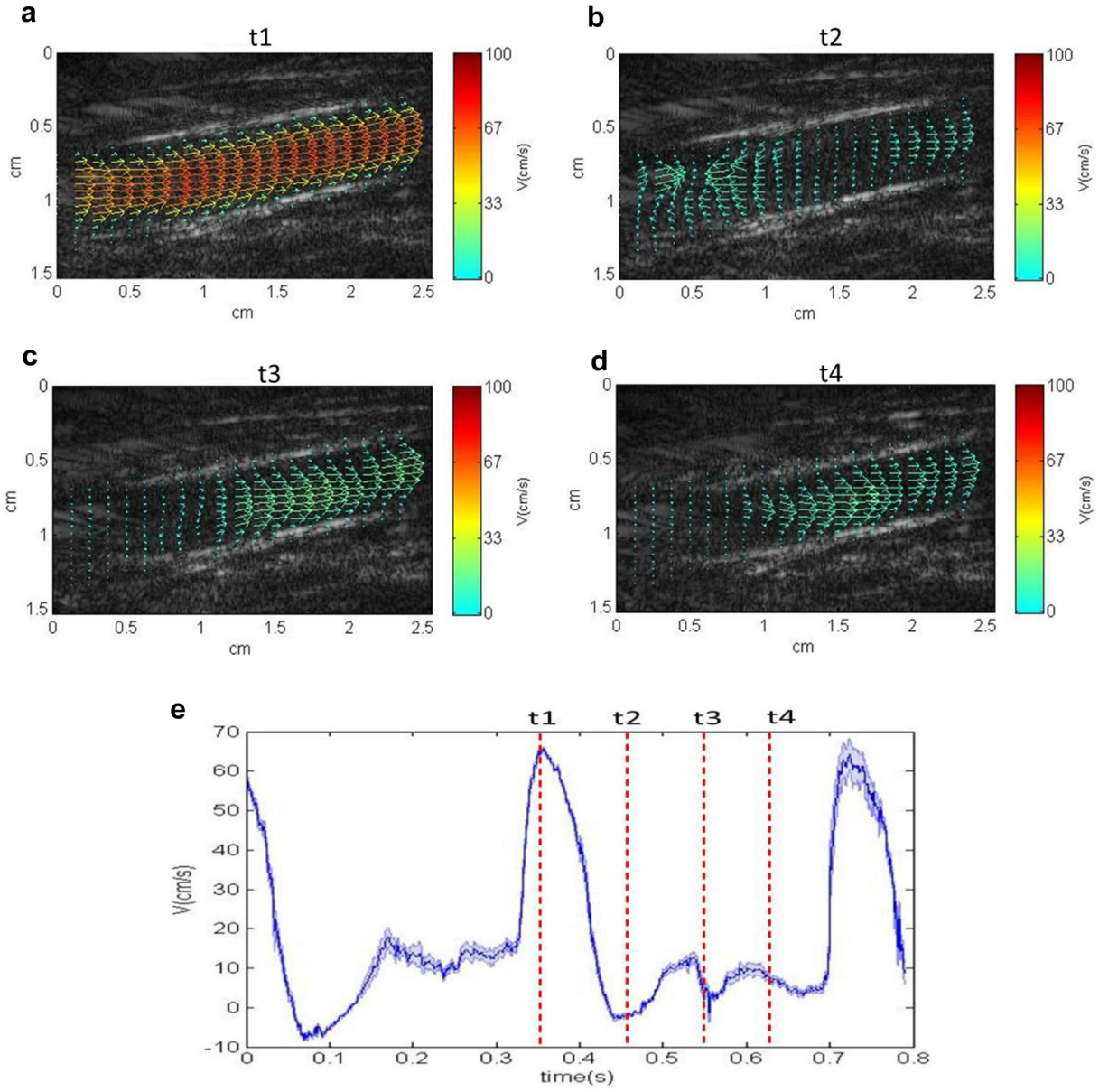

Fig. 9. (a–d) Quantitative visualisation of the flow patterns within a rabbit aorta. (e) Centreline velocity plot obtained using ultrasound imaging velocimetry from a 1 × 1-mm range gate within the aorta. The relative position of each flow pattern is marked in the velocity plot.

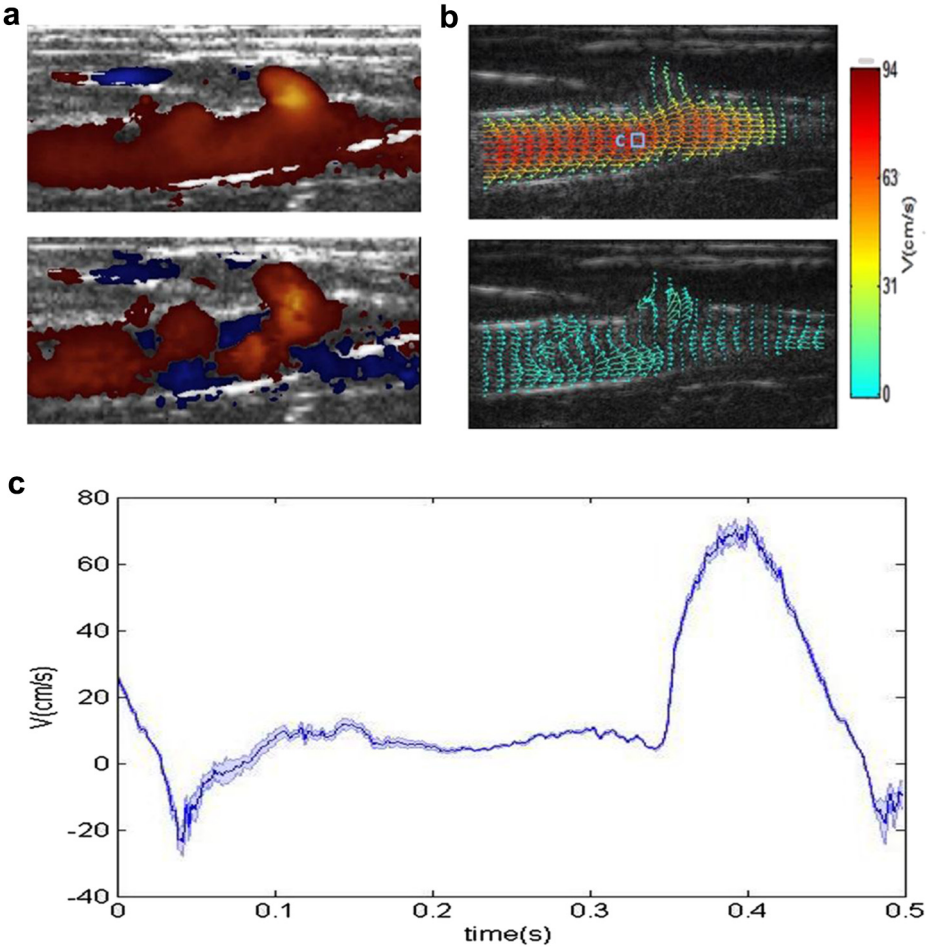

Fig. 10. Comparison of (a) a colour Doppler image, (b) quantitative visualisation of flow patterns estimated using ultrasound imaging velocimetry analysis and (c) centreline velocity extracted from a 1 × 1-mm range gate within the aorta shown in (b).

DISCUSSION

In this work, a high-frame-rate ultrasound UIV system and methodologies were developed for quantifying dynamic arterial flow, using plane wave ultrasound, microbubble contrast agents, pulse-inversion contrast imaging sequence and UIV algorithms. Initial *in vitro* evaluation on straight-vessel and carotid-mimicking phantoms, in comparison with both theoretical calculations and reference Doppler techniques, revealed the potential of the new system as an accurate, sensitive, angle-independent and full-field-of-view velocity mapping tool capable of tracking fast and dynamic flows.

The high temporal resolution of plane wave UIV, compared with existing line-by-line scanning, enables a much wider range of velocities to be measured using the speckle tracking approach. For example, given an imaging depth of 6.4 cm that enables a pulse repetition frequency of 12 kHz, as used in this study, a maximum frame rate of 2000 fps can be achieved with three-angled compounding and a pulse-inversion sequence. This is a 40-fold increase in frame rate, which enables the tracking of velocities up to 6 m/s compared with the conventional approach, in which the frame rate would be limited by the line-by-line scanning to a maximum of 50 fps when 128 scanning lines are used. It should also be noted that although a maximum temporal resolution of 12 kHz can be achieved if a single plane wave imaging approach is used, there is a trade-off between temporal resolution, spatial resolution and contrast image sensitivity.

Furthermore, plane wave imaging would allow a reduction in the errors that arise when determining flow velocity with line-by-line scanning and reported by Zhou et al. (2013); with the traditional approach, flow velocity is underestimated when the beam sweeping direction is opposite the flow direction and is overestimated when the beam sweeping direction is the same as the flow direction.

Microbubble contrast agents can enhance signals from within blood by 20–30 dB compared with blood

cells alone (Lencioni 2006). Hence, the use of microbubble contrast agents significantly improves the sensitivity of ultrasound imaging and, consequently, the accuracy of velocity estimation. This is particularly essential for imaging deep vessels/heart chambers where low-frequency ultrasound is required and blood cell scattering is much less than at high frequencies. The use of contrast-specific imaging sequences such as pulse inversion also allows better identification of blood–tissue boundaries and facilitates calculation of hemodynamic wall shear stress.

The capability of plane wave UIV to provide quantitative mapping of highly dynamic flows is illustrated in Supplementary Video 1 and Figure 7. The signal-to-noise ratio in the lumen is high, and the speckle patterns and their movement are clearly visible. With the acquisition rate (1000 fps) beyond normal display frame rate, we found that plane wave UIV was capable of resolving fast, spatiotemporally changing pulsatile flow. The evolution of flow patterns in a complete pulse cycle was accurately tracked by this technique. An additional advantage of using the plane wave UIV system was that temporal velocity profiles could be extracted from any place in the field of view. As illustrated in Figure 7(m), the extracted centreline velocity profile is strongly correlated with spectral Doppler measurements.

The advantage of using a plane wave UIV system to visualise complex flow dynamics within a physiologically relevant geometry was illustrated both *in vitro* and *in vivo*. The tracking of fast changes of flow in both space and time can be seen in Supplementary Videos 2 and 3 and Figures 8–10. Complex flow patterns in a complete pulse cycle—specifically the forward streamline flow and vortical flow at the carotid bulb in the phantom study, or forward and reversed streamline flow in the rabbit abdominal aorta—were illustrated. These transitory behaviours of the flow cannot be visualised with standard Doppler imaging, but were visible using high-frame-rate UIV.

In recent years, several flow measurement techniques that use high-frame-rate ultrasound imaging have emerged, including ultrafast Doppler, vector Doppler and ultrafast speckle tracking. Although these have exhibited improved performance over conventional ultrasound imaging systems, the use of a divergent or unfocussed beam and the weak scattering from the RBCs mean that the signal-to-noise ratios and contrast of these high-frame-rate ultrasound images are lower than those of conventional ultrasound images (Montaldo et al. 2009). This problem gets worse when lower frequencies need to be used in deeper vessel imaging. In this study, we used microbubbles contrast agents that can significantly increase signal-to-noise ratio from within blood. In comparison to conventional contrast imaging, the unfocussed beam of the plane wave imaging UIV system also reduces bubble disruption.

It should also be noted that the Doppler measurements, illustrated in Figures 6(d–f) and 7(m), were overestimates, likely because of the manual angle correction setting used clinically (Willink and Evans 1995) and the use of microbubbles, which widen the spectral measurement. Doppler spectral broadening can be attributed to the secondary radiation force when using high pulse repetition frequency; this has been investigated and discussed by Tortoli and colleagues (2005, 2009).

In the rabbit experiment, out-of-plane motion was observed, especially during the deceleration phase as the aorta contracts; this caused part of the 2-D image on the left-hand side to move from the lumen to the vessel wall, as illustrated in Figure 10(c, d). This is an inherent limitation of 2-D ultrasound in imaging 3-D structures and may well be resolved using 3-D ultrasound.

Although the developed high-frame-rate UIV system is capable of providing accurate quantification of the flow field, it can be further improved. Optimization of the ultrasound system parameters, such as the number of plane waves compounded, plane wave tilting angle, frequency, acoustic pressure, and pulse length, can enhance images and velocity estimation. For instance, the use of a small number of angles with large angle tilting to enhance spatial and temporal resolution in plane wave excitation can cause high grating lobes that could affect the accuracy of speckle tracking. Further investigation and optimization of the imaging parameters need to be conducted to balance the spatial and temporal resolution while optimizing tracking accuracy. In addition, it should be noted that the compounding required in plane wave imaging could cause the very fast flow dynamics to be missed; a trade-off has to be made between temporal resolution and spatial resolution. However, the benefit of the proposed method—ability to track a wide range of flow velocities within the whole imaging plane with great sensitivity and good spatial resolution—makes it an exciting addition to existing tools for flow imaging and quantification.

The proposed technique is capable of producing over time a spatially resolved flow velocity map containing a large amount of data. In this study, as an example of what can be extracted, a temporal velocity profile at a single location within the vessel is provided for the carotid phantom (Figs. 7m and 8g) and the rabbit abdominal aorta *in vivo* (Figs. 9e and 10c). Further hemodynamic indices that could be derived from the data include not only the existing indices obtained by Doppler, such as peak and average velocities and flow pulsatility, but also quantities related to spatial variation of the flow velocity, such as flow vorticity and local wall shear rate.

Furthermore, real-time processing using a graphics processing unit is also desirable to provide an immediate quantitative measurement for clinical applications. Finally, this study uses a 2-D imaging system that is not capable of tracking out-of-plane flow. For future *in vivo* applications, a 3-D imaging approach would need to be developed.

CONCLUSIONS

The developed quantitative flow mapping system, integrating high-frame-rate plane wave imaging, ultrasound imaging velocimetry and microbubble contrast agents, has great potential as an accurate, sensitive, angle-independent and full-field-of-view velocity measuring tool capable of mapping fast and dynamic flows *in vivo*.

The technique could potentially be used in a wide range of research and clinical applications, such as studying the flows and resulting wall shear stresses that determine the initiation and development of vascular lesions such as atherosclerosis, and clinically evaluating the lesions. The system also has great potential in mapping flow within heart chambers, providing a more accurate and quantitative measurement of heart function and shunts.

Acknowledgments—Meng-Xing Tang acknowledges the funding from EPSRC (EP/M011933/1 & EP/K503733/1). C.H. Leow is supported by Postgraduate Research Scholarship from the Public Service Department of Malaysia. Peter Weinberg and Eleni Bazigou acknowledges the funding from British Heart Foundation (P35424). Alfred C.H. Yu acknowledges the Research Grants Council of Hong Kong (GRF 785811M).

SUPPLEMENTARY DATA

Supplementary data related to this article can be found at http://dx.doi.org/10.1016/j.ultrasmedbio.2015.06.012.

REFERENCES

Adrian RJ. Particle-imaging techniques for experimental fluid mechanics. Annu Rev Fluid Mech 1991;23:261–304.
Adrian RJ, Westerweel J. Particle image velocimetry. London/New York: Cambridge University Press; 2011.
Bercoff J, Montaldo G, Loupas T, Savery D, Meziere F, Fink M, Tanter M. Ultrafast compound Doppler imaging: Providing full blood flow characterization. IEEE Trans Ultrason Ferroelectr Freq Control 2011;58:134–147.
Bohs LN, Geiman BJ, Anderson ME, Gebhart SC, Trahey GE. Speckle tracking for multi-dimensional flow estimation. Ultrasonics 2000; 38:369–375.
Cecchi E, Giglioli C, Valente S, Lazzeri C, Gensini GF, Abbate R, Mannini L. Role of hemodynamic shear stress in cardiovascular disease. Atherosclerosis 2011;214:249–256.
Couture O, Bannouf S, Montaldo G, Aubry JF, Fink M, Tanter M. Ultrafast imaging of ultrasound contrast agents. Ultrasound Med Biol 2009;35:1908–1916.
Davies PF. Hemodynamic shear stress and the endothelium in cardiovascular pathophysiology. Nat Clin Pract Cardiovasc Med 2009;6: 16–26.
Ekroll IK, Swillens A, Segers P, Dahl T, Torp H, Lovstakken L. Simultaneous quantification of flow and tissue velocities based on multi-angle plane wave imaging. IEEE Trans Ultrason Ferroelectr Freq Control 2013;60:727–738.
Evans DH, Jensen JA, Nielsen MB. Ultrasonic colour Doppler imaging. Interface Focus 2011;1:490–502.
Evans DH, Wells PNT. Colour flow and motion imaging. Proc Inst Mech Eng [H] 2010;224:241–253.
Fadnes S, Nyrnes SA, Torp H, Lovstakken L. Shunt flow evaluation in congenital heart disease based on two-dimensional speckle tracking. Ultrasound Med Biol 2014;40:2379–2391.
Ferrara K, Pollard R, Borden M. Ultrasound Microbubble Contrast Agents: Fundamentals and Application to Gene and Drug Delivery. Annu Rev Biomed Eng 2007;9:415–447.
Flynn J, Daigle R, Pflugrath L, Kaczkowski P. High frame rate vector velocity blood flow imaging using a single plane wave transmission angle. Proc IEEE Int Ultrason Symp 2012;323–325.
Gülan U, Lüthi B, Holzner M, Liberzon A, Tsinober A, Kinzelbach W. Experimental study of aortic flow in the ascending aorta via Particle Tracking Velocimetry. Exp Fluids 2012;53:1469–1485.
He X, Ku DN. Unsteady entrance flow development in a straight tube. J Biomech Eng 1994;116:355–360.
Hoskins P. Peak velocity estimation in arterial stenosis models using colour vector Doppler. Ultrasound Med Biol 1997;23:889–897.
Jensen J, Nikolov S. Directional synthetic aperture flow imaging. IEEE Trans Ultrason Ferroelectr Freq Control 2004;51:1107–1118.
Jensen JA, Lacasa IR. Estimation of blood velocity vectors using transverse ultrasound beam focusing and cross-correlation. Proc IEEE Int Ultrason Symp 1999;1493–1497.
Jensen JA, Nikolov SI, Gammelmark KL, Pedersen MH. Synthetic aperture ultrasound imaging. Ultrasonics 2006;44:e5–e15.
Kortbek J, Jensen J. Estimation of velocity vector angles using the directional cross-correlation method. IEEE Trans Ultrason Ferroelectr Freq Control 2006;53:2036–2049.
Kripfgans OD, Rubin JM, Hall AL, Fowlkes JB. Vector Doppler imaging of a spinning disc ultrasound Doppler phantom. Ultrasound Med Biol 2006;32:1037–1046.
Ku DN. Blood flow in arteries. Annu Rev Fluid Mech 1997;29:399–434.
Lai SSM, Yiu BYS, Poon AKK, Yu ACH. Design of anthropomorphic flow phantoms based on rapid prototyping of compliant vessel geometries. Ultrasound Med Biol 2013;39:1654–1664.
Lencioni R. Enhancing the role of ultrasound with contrast agents. Milan/Berlin: Springer; 2006.
Lenge M, Ramalli A, Cellai A, Tortoli P, Cachard C, Liebgott H. A new method for 2 D-vector blood flow imaging based on unconventional beamforming techniques. Proc IEEE Int Conf Acoust Speech Signal Process 2014;5125–5129.
Lindner JR. Microbubbles in medical imaging: Current applications and future directions. Nat Rev Drug Discov 2004;3:527–533.
Lindner JR. Molecular imaging of cardiovascular disease with contrast-enhanced ultrasonography. Nat Rev Cardiol 2009;6:475–481.
McDonald D. Blood flow in arteries. 2nd ed. London: Edward Arnold; 1974.
Montaldo G, Tanter M, Bercoff J, Benech N, Fink M. Coherent plane-wave compounding for very high frame rate ultrasonography and transient elastography. IEEE Trans Ultrason Ferroelectr Freq Control 2009;56:489–506.
Mulvana H, Stride E, Tang M-X, Hajnal JV, Eckersley RJ. The influence of gas saturation on microbubble stability. Ultrasound Med Biol 2012;38:1097–1100.
Nam KH, Yeom E, Ha H, Lee SJ. Velocity field measurements of valvular blood flow in a human superficial vein using high-frequency ultrasound speckle image velocimetry. Int J Cardiovasc Imaging 2012;28:69–77.
Niu L, Qian M, Wan K, Yu W, Jin Q, Ling T, Gao S, Zheng H. Ultrasonic particle image velocimetry for improved flow gradient imaging: Algorithms, methodology and validation. Phys Med Biol 2010;55: 2103–2120.
Ohtsuki S, Tanaka M. The flow velocity distribution from the Doppler information on a plane in three-dimensional flow. J Vis 2006;9: 69–82.

Pastorelli A, Torricelli G, Scabia M, Biagi E, Masotti L. A real-time 2-D vector Doppler system for clinical experimentation. IEEE Trans Med Imaging 2008;27:1515–1524.

Pedersen MM, Pihl MJ, Haugaard P, Hansen KL, Lange T, Lönn L, Nielsen MB, Jensen JA. Novel flow quantification of the carotid bulb and the common carotid artery with vector flow ultrasound. Ultrasound Med Biol 2014;40:2700–2706.

Poelma C, Mari JM, Foin N, Tang MX, Krams R, Caro CG, Weinberg PD, Westerweel J. 3D Flow reconstruction using ultrasound PIV. Exp Fluids 2009;50:777–785.

Poelma C, van der Mijle RME, Mari JM, Tang MX, Weinberg PD, Westerweel J. Ultrasound imaging velocimetry: Toward reliable wall shear stress measurements. Eur J Mech B/Fluids 2012;35:70–75.

Qian M, Niu L, Wang Y, Jiang B, Jin Q, Jiang C, Zheng H. Measurement of flow velocity fields in small vessel-mimic phantoms and vessels of small animals using micro ultrasonic particle image velocimetry (micro-EPIV). Phys Med Biol 2010;55:6069–6088.

Ramnarine KV, Nassiri DK, Hoskins PR, Lubbers J. Validation of a new blood-mimicking fluid for use in Doppler flow test objects. Ultrasound Med Biol 1998;24:451–459.

Reneman RS, Arts T, Hoeks APG. Wall shear stress—an important determinant of endothelial cell function and structure—in the arterial system in vivo. J Vasc Res 2006;43:251–269.

Ricci S, Bassi L, Tortoli P. Real-time vector velocity assessment through multigate Doppler and plane waves. IEEE Trans Ultrason Ferroelectr Freq Control 2014;61:314–324.

Sboros V, Tang M-X, Wells PNT. The assessment of microvascular flow and tissue perfusion using ultrasound imaging. Proc Inst Mech Eng [H] 2010;224:273–290.

Sennoga CA, Yeh JSM, Alter J, Stride E, Nihoyannopoulos P, Seddon JM, Haskard DO, Hajnal JV, Tang MX, Eckersley RJ. Evaluation of methods for sizing and counting of ultrasound contrast agents. Ultrasound Med Biol 2012;38:834–845.

Sheeran PS, Luois S, Dayton PA, Matsunaga TO. Formulation and acoustic studies of a new phase-shift agent for diagnostic and therapeutic ultrasound. Langmuir 2011;27:10412–10420.

Simpson DH, Chin CT, Burns PN. Pulse inversion Doppler: A new method for detecting nonlinear echoes from microbubble contrast agents. IEEE Trans Ultrason Ferroelectr Freq Control 1999;46:372–382.

Steel R, Ramnarine KV, Davidson F, Fish PJ, Hoskins PR. Angle-independent estimation of maximum velocity through stenoses using vector Doppler ultrasound. Ultrasound Med Biol 2003;29:575–584.

Stride E, Tang MX, Eckersley RJ. Physical phenomena affecting quantitative imaging of ultrasound contrast agents. Appl Acoust 2009;70:1352–1362.

Stride EP, Coussios CC. Cavitation and contrast: the use of bubbles in ultrasound imaging and therapy. Proc Inst Mech Eng [H] 2010;224:171–191.

Swillens A, Segers P, Lovstakken L. Two-dimensional flow imaging in the carotid bifurcation using a combined speckle tracking and phase-shift estimator: A study based on ultrasound simulations and in vivo analysis. Ultrasound Med Biol 2010a;36:1722–1735.

Swillens A, Segers P, Torp H, Lovstakken L. Two-dimensional blood velocity estimation with ultrasound: speckle tracking versus crossed-beam vector Doppler based on flow simulations in a carotid bifurcation model. IEEE Trans Ultrason Ferroelectr Freq Control 2010b;57:327–339.

Tang MX, Kamiyama N, Eckersley RJ. Effects of nonlinear propagation in ultrasound contrast agent imaging. Ultrasound Med Biol 2010;36:459–466.

Tang MX, Mulvana H, Gauthier T, Lim AKP, Cosgrove DO, Eckersley RJ, Stride E. Quantitative contrast-enhanced ultrasound imaging: A review of sources of variability. Interface Focus 2011;1:520–539.

Tanter M, Fink M. Ultrafast imaging in biomedical ultrasound. IEEE Trans Ultrason Ferroelectr Freq Control 2014;61:102–119.

Tortoli P, Boni E, Corsi M, Arditi M, Frinking P. Different effects of microbubble destruction and translation in Doppler measurements. IEEE Trans Ultrason Ferroelectr Freq Control 2005;52:1183–1188.

Tortoli P, Dallai A, Boni E, Francalanci L, Ricci S. An automatic angle tracking procedure for feasible vector Doppler blood velocity measurements. Ultrasound Med Biol 2010;36:488–496.

Tortoli P, Guidi F, Mori R, Vos HJ. The use of microbubbles in Doppler ultrasound studies. Med Biol Eng Comput 2009;47:827–838.

Tremblay-Darveau C, Williams R, Milot L, Bruce M, Burns PN. Combined perfusion and Doppler imaging using plane-wave nonlinear detection and microbubble contrast agents. IEEE Trans Ultrason Ferroelectr Freq Control 2014;61:1988–2000.

Udesen J, Jensen JA. Investigation of transverse oscillation method. IEEE Trans Ultrason Ferroelectr Freq Control 2006;53:959–971.

Uejima T, Koike A, Sawada H, Aizawa T, Ohtsuki S, Tanaka M, Furukawa T, Fraser AG. A new echocardiographic method for identifying vortex flow in the left ventricle: Numerical validation. Ultrasound Med Biol 2010;36:772–788.

Westerweel J, Scarano F. Universal outlier detection for PIV data. Exp Fluids 2005;39:1096–1100.

Willink R, Evans DH. Volumetric blood flow calculation using a narrow ultrasound beam. Ultrasound Med Biol 1995;21:203–216.

Yamaguchi T, Kikkawa S, Parker K. Simulation of nonstationary spectral analysis of turbulence in the aorta using a modified autoregressive or maximum entropy (ar/me) method. Med Biol Eng Comput 1987;25:533–542.

Yeom E, Nam KH, Paeng DG, Lee SJ. Improvement of ultrasound speckle image velocimetry using image enhancement techniques. Ultrasonics 2014;54:205–216.

Yim P, DeMarco K, Castro MA, Cebral J. Characterization of shear stress on the wall of the carotid artery using magnetic resonance imaging and computational fluid dynamics. Stud Health Technol Inform 2005;113:412–442.

Yiu BYS, Lai SSM, Yu ACH. Vector projectile imaging: Time-resolved dynamic visualization of complex flow patterns. Ultrasound Med Biol 2014;40:2295–2309.

Zhang F, Lanning C, Mazzaro L, Barker AJ, Gates PE, Strain WD, Fulford J, Gosling OE, Shore AC, Bellenger NG, Rech B, Chen J, Chen J, Shandas R. *In vitro* and preliminary *in vivo* validation of echo particle image velocimetry in carotid vascular imaging. Ultrasound Med Biol 2011;37:450–464.

Zhou B, Fraser KH, Poelma C, Mari J-M, Eckersley RJ, Weinberg PD, Tang MX. Ultrasound Imaging velocimetry: Effect of beam sweeping on velocity estimation. Ultrasound Med Biol 2013;39:1672–1681.